



HAL
open science

First identification of a Cathaysian continental fragment beneath the Gagua Ridge, Philippine Sea, and its tectonic implications

Shengping Qian, Xiaozhi Zhang, Jonny Wu, Serge Lallemand, Alexander R.L. Nichols, Chiyue Huang, Daniel P Miggins, Huaiyang Zhou

► To cite this version:

Shengping Qian, Xiaozhi Zhang, Jonny Wu, Serge Lallemand, Alexander R.L. Nichols, et al.. First identification of a Cathaysian continental fragment beneath the Gagua Ridge, Philippine Sea, and its tectonic implications. *Geology*, 2021, 49, 10.1130/G48956.1 . hal-03362061

HAL Id: hal-03362061

<https://hal.science/hal-03362061>

Submitted on 8 Oct 2021

HAL is a multi-disciplinary open access archive for the deposit and dissemination of scientific research documents, whether they are published or not. The documents may come from teaching and research institutions in France or abroad, or from public or private research centers.

L'archive ouverte pluridisciplinaire **HAL**, est destinée au dépôt et à la diffusion de documents scientifiques de niveau recherche, publiés ou non, émanant des établissements d'enseignement et de recherche français ou étrangers, des laboratoires publics ou privés.

1 **First identification of a Cathaysian continental**
2 **fragment beneath the Gagua Ridge, Philippine Sea,**
3 **and its tectonic implications**

4

5 Shengping Qian^{1**}, Xiaozhi Zhang^{1#}, Jonny Wu², Serge Lallemand³, Alexander R.
6 L. Nichols⁴, Chiyue Huang^{1,5}, Daniel P. Miggins⁶, Huaiyang Zhou^{1*}

7

8 *¹State Key Laboratory of Marine Geology, Tongji University, Shanghai 200092,*
9 *China*

10 *²Department of Earth & Atmospheric Sciences, University of Houston, Houston,*
11 *Texas 77204, USA*

12 *³Géosciences Montpellier, CNRS, Montpellier University, 34095 Montpellier cédex 5,*
13 *France*

14 *⁴School of Earth and Environment, University of Canterbury, Christchurch 8140, New*
15 *Zealand*

16 *⁵Department of Earth Sciences, National Cheng Kung University, 701 Tainan, Taiwan*

17 *⁶College of Earth, Ocean and Atmospheric Sciences, Oregon State University,*
18 *Corvallis, OR 97331, USA*

19

20 * Corresponding author: shengpingqian@tongji.edu.cn, zhouhy@tongji.edu.cn

21 1239 Siping road, Shanghai, China, 021-20926959

22 # Co-first author

23

24 **ABSTRACT**

25 The tectonic history of the Philippine Sea Plate is essential to understand the
26 tectonic evolution of Southeast Asia, but it is still unclear and controversial. Here, we
27 present the first geochemical data of lavas from the Gagua Ridge (GR) within the
28 Philippine Sea. The GR lavas exhibit geochemical signatures typical of
29 subduction-related arc magmatism. Plagioclase Ar-Ar ages of ~123-124 Ma, as well as
30 subduction-related geochemical signatures, support the formation of GR lavas in the
31 vicinity of an arc during the Early Cretaceous induced by subduction of the oceanic
32 plate along East Asia. The ages of trapped zircon xenocrysts within the GR lavas cluster
33 at 250 Ma, 0.75 Ga and 2.45 Ga, and match well the ages of zircons recovered from the
34 Cathaysian block, South China. Our results imply that the GR basement is partially
35 comprised of continental material that rifted away from the Eurasian margin during
36 opening and spreading of the Huatung Basin (HB). The depleted mantle wedge-derived
37 magmas evolved and picked up the continental zircons during ascent. The youngest
38 zircon ages and the GR lava Ar-Ar ages (~123-124 Ma) presented in this study newly
39 constrain an Early Cretaceous age for the HB. Our study provides further evidence that
40 the HB is a remnant of a Mesozoic-aged ocean basin that dispersed from South China
41 during the Cretaceous. Transport of continental slivers by growth and closure of

42 marginal seas along the East Asia margin may have been more prevalent than
43 previously recognized.

44

45 **INTRODUCTION**

46 The Philippine Sea Plate (PSP) is composed of a mosaic of marginal basins, and
47 is almost completely bounded by subduction zones that involve the
48 Eurasian/Sundaland plates to the west, the Pacific Plate to the east, and the
49 Indo-Australian Plate to the south (e.g. Hall, 2002). Tectonic studies of the PSP have a
50 profound influence on the origin of marginal seas, and plate tectonic reconstructions
51 for vast areas of Southeast (SE) China, SE Asia and western Pacific regions since the
52 Cretaceous (Hilde and Lee, 1984; Hall, 2002; Sibuet et al., 2002; Hsu and
53 Deffontaines, 2009; Zahirovic et al., 2014; Lallemand, 2016; Wu et al., 2016; Huang
54 et al., 2019). Although some portions of the PSP are better-studied and show oceanic
55 basins and ocean island arc lithosphere of Early Cretaceous to recent ages
56 (Deschamps and Lallemand, 2002; Taylor and Goodliffe, 2004; Hickey-Vargas et al.,
57 2008; Tani et al., 2011), other areas are completely undrilled and remain enigmatic.
58 One such region is the Huatung Basin (HB) and the Gagua Ridge (GR) along the
59 northwestern PSP (**Fig. 1**), the focus of this study.

60 The northwestern PSP is composed of two ocean basins: the larger and
61 better-studied West Philippine Basin (WPB), and the undrilled, smaller HB (**Fig. 1**).
62 The GR is a bathymetric high between the HB and WPB, occupying a unique position

63 **(Fig. 1)**. Existing interpretations regarding the origin of the GR are diverse, including
64 an uplifted sliver of oceanic crust (Mrozowski et al., 1982), a former intraoceanic
65 fracture zone (Deschamps et al., 1998), WPB-HB plate boundary (Deschamps et al.,
66 2000; Sibuet et al., 2002), or a relict subduction zone (i.e. westward subduction of the
67 WPB beneath the HB along the GR) (Deschamps and Lallemand, 2002; Eakin et al.,
68 2015). Each scenario has wide-ranging implications for HB-WPB interactions and SE
69 Asian plate tectonic evolution and is explored in this study.

70 Here, we present new Ar-Ar geochronology and geochemistry for GR lavas:
71 major and trace element, and Sr-Nd-Hf-Pb isotope data for the whole rocks; and
72 U-Pb-Hf isotopic and trace element data for zircons from the lavas. Combined with
73 the regional tectonic constraints, our study provides new insights into the nature,
74 origin and dispersal of the GR that elucidate the tectonic evolution of SE Asia.

75

76 **GEOLOGICAL SETTING AND SAMPLES**

77 The HB is a small ocean basin that has an enigmatic tectonic history. Deschamps
78 and Lallemand (2002) proposed that the HB was near-equatorial in the early Cenozoic
79 and then docked against the adjacent WPB along the GR around ~35 Ma, while Hall
80 (2012) considers the HB to have been near ~20°N latitudes for most of its history. If
81 the HB and Luzon were already juxtaposed by the Eocene, Luzon paleomagnetism
82 similarly places the HB near the equator or even at low latitudes within the southern
83 hemisphere during the Eocene (Queano et al., 2007). Wu et al. (2016) follows Queano

84 et al. (2007) and reconstructs Luzon-HB to be within the now-vanished marginal
85 'East Asia Sea'.

86 The GR is adjacent to an unusual subduction flipping system (e.g. the PSP
87 subducting northwestward along the Ryukyu Trench, and the South China Sea (SCS)
88 subducting eastward along the Manila Trench) (Angelier, 1986; Sibuet et al., 2002)
89 (**Fig. 1**). The geophysical data indicates crustal thickening on the order of ~12–18 km
90 beneath the GR (Eakin et al., 2015). Besides, the northernmost segment of this linear
91 GR subducts beneath the Ryukyu trench (Deschamps et al., 1998; Dominguez et al.,
92 1998).

93 Lavas were collected from the GR by ROV Haixing6000 (**Fig. 1**). Four sites
94 around the highest peak of the ridge were investigated but only those located at the top
95 provided relatively fresh volcanic rocks (**Fig. DR1 and DR2A**). The lavas are massive
96 and porphyritic, containing clinopyroxene, plagioclase and orthopyroxene phenocrysts
97 (**Fig. DR2C and D**). Some plagioclases have resorption textures, leaving incomplete
98 and crooked rims (**Fig. DR2D**).

99 Detailed petrography of samples, analytical methods, analytical data, and data
100 plots are provided in the supplementary material.

101

102 **RESULTS**

103 The zircons from the GR lavas show an age spectrum mainly ranging from
104 Cretaceous to Archean, with three prominent population peaks at 250 Ma (n=13), 750

105 Ma (n=24), and 2450 Ma (n=14) (**Fig. 2B**). The zircons display a wide range of $\epsilon_{\text{Hf}}(t)$
106 values, from -31.0 to 23.8 (**Fig. 2A**), corresponding to highly variable crustal model
107 ages (T_{DM}^C) between ca. 382 Ma and 3015 Ma (**Table DR4**), consistent with a
108 heterogenous source. Plagioclases in the GR lavas yielded weighted Ar-Ar mean ages
109 of 123.99 ± 0.24 Ma and 124.06 ± 0.27 Ma (**Fig. 2E, F**).

110 Generally, the GR lavas show a limited variation in major elements (e.g., SiO₂:
111 54.38–56.21 wt.%, total alkalis: 4.32–5.87 wt.%), and are mainly basaltic andesites
112 (**Fig. 3A**). They are characterized by the enrichment of large ion lithophile elements
113 (LILEs, e.g. Ba, U, K and Pb), resembling the signature of subduction-related rocks
114 from circum-Pacific arcs (**Fig. 3B**). They all display depleted mantle-type isotopic
115 signatures, with low $^{87}\text{Sr}/^{86}\text{Sr}$ (0.703297–0.703574), and high $^{143}\text{Nd}/^{144}\text{Nd}$ (0.512972–
116 0.513067) and $^{176}\text{Hf}/^{177}\text{Hf}$ (0.283112–0.283157) (**Fig. 3F, G, H**). The GR lavas show a
117 limited range of Pb isotope compositions ($^{206}\text{Pb}/^{204}\text{Pb} = 18.279\text{--}18.330$, $^{207}\text{Pb}/^{204}\text{Pb} =$
118 $15.476\text{--}15.493$, and $^{208}\text{Pb}/^{204}\text{Pb} = 37.961\text{--}38.038$) (**Fig. 3E and Table DR1**).

119

120 CONTINENTAL FRAGMENT BENEATH THE GR

121 U-Pb ages of zircons in the GR lavas range widely from 123 to 3035 Ma (**Fig.**
122 **2A, B**), which suggests that zircon grains are likely xenocrystic. The GR zircons have
123 high U, Th and Y contents and U/Yb values that markedly differ from those of
124 recycled oceanic crust, mantle peridotite and kimberlite, but resemble those of
125 continental crust (**Fig. 2C, D**). The U-Pb ages and Hf isotope systematics of the GR

126 zircons (**Fig. 2A, B**) broadly match those of zircon records from the Cathaysian block,
127 South China (Yu et al., 2010; Li et al., 2014). The Mesozoic age peak (250 Ma) of the
128 GR zircons can possibly be related to widespread contemporaneous magmatic rocks
129 in South China, while zircon age peaks (~ 0.75 Ga and ~ 2.45 Ga) are largely
130 consistent with those for zircons from Cathaysia crust, South China (**Fig. 2B**). Thus,
131 the GR zircons most likely originated from Cathaysian Block.

132 The GR zircons are likely inherited from crust-derived material within mantle
133 sources. It is known that crust-derived materials only contain small amounts of
134 accessory zircon. If our zircon xenocrysts are derived from recycled continental crust
135 in the mantle source, the erupted lavas would have continental signatures, e.g.,
136 enriched Sr-Nd isotope, due to significantly higher trace element contents of recycled
137 continental crust relative to mantle. However, these features are absent in the GR
138 lavas (e.g. the depleted mantle-like Sr-Nd isotopic compositions) (**Fig. 3F**).
139 Furthermore, inherited zircons with multiple episodes of recycling and/or long-
140 distance transport are typically well rounded or ellipsoidal with pitted surfaces. In
141 contrast, most of the inherited zircons in the GR lavas are euhedral to subhedral (**Fig.**
142 **DR3**), suggesting no long-distance transport. All the above features argue against the
143 GR zircons being from subducting sediment involving long transport distances or
144 from crust with multiple episodes of recycling.

145 Alternatively, the zircons in the GR lavas could have been entrained from the
146 Cathaysian crust during magma ascent and/or within the magma chamber. This

147 implies the existence of continental crust beneath the GR. Compared to older
148 continental crust, the GR lavas have remarkably depleted Sr-Nd isotope compositions
149 (**Fig. 3F**), which suggests that juvenile parent magmas assimilated a small amount of
150 older material to incorporate zircon grains but not enough to dramatically affect
151 isotopic systematics.

152

153 **PETROGENESIS**

154 As shown in a multi-element spider diagram (**Fig. 3B**), enrichments in
155 fluid-mobile elements (e.g., U, K, Pb, Sr and Ba) of the GR lavas are typical of
156 subduction-related magmatism. The relatively low Ti/V, as well as high Ba/Yb, of the
157 GR lavas represent subduction-related signatures (**Fig. 3C, D**). Unlike mature arc
158 systems (e.g. Luzon and Ryukyu Arc), the isotopic compositions of the GR lavas plot
159 far away from the domain of global subducting sediment (GLOSS, Plank and Langmuir,
160 1998) (**Fig. 3E, F, G**). In particular, the GR lavas are distributed along the mantle array
161 on the plot of $^{143}\text{Nd}/^{144}\text{Nd}$ versus $^{176}\text{Hf}/^{177}\text{Hf}$ (**Fig. 3H**), suggesting fairly minor
162 contribution from subducting sediment to the mantle source (Plank and Langmuir,
163 1998; Hickey-Vargas et al., 2008). Additionally, the GR lavas have a typical
164 subducted slab-derived 'fluid' signature with low Nd/Pb (<4.3 relative to ~20 in
165 mid-ocean ridge basalts) (**Fig. 3E**). In the case of the GR lavas, the elevations of
166 Sr/Th and Ba/La, coupled with the narrow variations of Th/Ce and Th/Yb (**Fig. DR4**)
167 also underline a significant contribution of slab-derived fluids to the mantle source.

168 Consequently, we postulate that the GR lavas are derived from depleted mantle that
169 had been metasomatized by subducted slab-related materials. Following the approach
170 of Ishizuka et al. (2003), a simple simulation shows that the mantle source of the GR
171 lavas was likely to be metasomatized by ~4% fluid derived from altered oceanic crust
172 (AOC) and subducted sediment in a mixing ratio of 50:50 to 90:10 (**Fig. 3F and G**).

173 The GR lavas show subduction-related arc geochemical signatures, suggesting a
174 past subduction event. The GR lavas formed by 124 Ma (**Fig. 2E, F**), which is also
175 consistent with the minimum age (123 ± 1.7 Ma) of zircon in the GR lavas within
176 error (**Table DR2**). Thus, it is most likely that the GR lavas are derived from a mantle
177 source region metasomatised by slab-derived fluids along South China during the
178 Cretaceous, which was an active margin (e.g. Hall, 2012). In terms of geochemical
179 compositions, the HB lavas have compositions similar to lavas formed in back-arc
180 basin and spreading centers (e.g., Nb, Ta and Ti enrichments, relatively high Nd/Pb
181 and Ti/V, and low Ba/Yb, **Fig. 3**), while the GR lavas are more influenced by
182 subducted components (the arc or close to rear-arc position).

183

184 **IMPLICATIONS FOR SE ASIA TECTONIC EVOLUTION**

185 Published geophysical and geochemical data, sedimentation rates, and
186 geomagnetic modeling, show that the HB is likely a trapped remnant of
187 Cretaceous-aged oceanic basin (Deschamps et al., 2000; Hickey-Vargas et al., 2008;
188 Eakin et al., 2015; Huang et al., 2019; Hsieh et al., 2020). However, other studies

189 favor a younger age for the HB based on seafloor magnetics and seismology,
190 including Eocene (Hilde and Lee, 1984), Eocene to Miocene (Sibuet et al., 2002),
191 Oligo-Miocene (Kuo et al., 2009), or mid-late Eocene (Doo et al., 2014). Our study
192 affirms a Cretaceous age for the HB based on our GR lava eruption ages and the
193 youngest zircon ages of ~123-124 Ma (**Fig. 2 and Table DR2**).

194 Our identification of a Cathaysian continental fragment in the Philippine Sea
195 suggests that HB formation could be related to rifting of the Cathaysian Block during
196 the Cretaceous, when SE China transitioned from an active subducting margin to
197 extension (Xu et al., 2014; Zahirovic et al., 2016). It is also possible that the HB
198 formed during the Early Cretaceous from 131 to 119 Ma (Deschamps et al., 2000);
199 both cases imply rifting of a Cathaysian continental fragment during the Cretaceous.
200 Combining published plate models with our results, the HB could be either
201 far-traveled or remained relatively close to Eurasia during its history (**Fig. 4**). In the
202 far-traveled scenario, the HB was located near South China in the Early Cretaceous,
203 drifted ~2000 km southwards to equatorial latitudes by the Eocene, and then followed
204 the PSP and Luzon ~2000 km northwards after 50 Ma to its present position (**Fig. 4**).
205 Southward drift of the HB could be accommodated by opening of a backarc basin or
206 marginal sea near South China, including a large proto-SCS or other vanished
207 marginal seas (Deschamps and Lallemand, 2002; Wu et al., 2016; Zahirovic et al.,
208 2016). Alternatively, a ‘short transport’ scenario is possible where the HB is a relict
209 proto-SCS fragment that remained relatively close to South China, moved ~500 km

210 southwards during the SCS opening, was captured by the PSP and then moved ~500
211 km northwards (**Fig. 4**) (Hall, 2012). This scenario requires the HB to be tectonically
212 transported a shorter distance and seems more favorable (**Fig. 4**), and is still
213 compatible within specific constraints used by far-traveled plate models (Deschamps
214 and Lallemand, 2002; Wu et al., 2016).

215 Another sliver of Cathaysian-affinity continent has been found within the Luzon
216 Arc basement that apparently drifted southwards during the SCS opening, was
217 accreted and then moved northwards with the PSP during the mid- to late Cenozoic
218 (Shao et al., 2015). Taken together, we newly present the undrilled HB as a narrow
219 (up to 150 km wide) sliver of oceanic crust, bounded on both sides by continental
220 fragments of Cathaysian-affinity (**Fig. 4**). Accretion of ‘ribbon continents’ is
221 fundamental in orogenesis and continental growth over time and space (Cawood et al.,
222 2009). Our results now show that the transport of continental slivers by growth and
223 closure of marginal seas along the East Asia margin (**Fig. 4**) may be more prevalent
224 than previously recognized.

225

226 **ACKNOWLEDGMENTS**

227 This study was supported by the National Natural Science Foundation (NSF) of China
228 (41902044 and 91428207) and the Chinese National Key Basic Research Program
229 (2012CB417300). Jonny Wu was supported by US NSF grant EAR-1848327. We thank
230 editor Prof. Gerald Dickens, reviewer Sabin Zahirovic, and two anonymous reviewers

231 for their constructive and helpful reviews. Stéphane Dominguez is thanked for
232 providing the bathymetric compilation. Shenyang Institute of automation and Zhiguo
233 Qiao are thanked for helping collect the sample. We thank Le Zhang for assistance in
234 the sample analysis.

235

236 REFERENCES CITED

- 237 Angelier, J., 1986, Geodynamics of the Eurasia-Philippine Sea plate boundary:
238 preface: *Tectonophysics*, v. 125, no. 1, p. IX-X,
239 doi.org/10.1016/0040-1951(86)90003-X.
- 240 Cawood, P. A., Kröner, A., Collins, W. J., Kusky, T. M., Mooney, W. D., and Windley,
241 B. F., 2009, *Accretionary orogens through Earth history*: Geological Society,
242 London, Special Publications, v. 318, no. 1, p. 1-36, doi:10.1144/sp318.1.
- 243 Deschamps, A., and Lallemand, S., 2002, The West Philippine Basin: An Eocene to
244 early Oligocene back arc basin opened between two opposed subduction zones:
245 *Journal of Geophysical Research*, v. 107, doi:10.1029/2001JB001706.
- 246 Deschamps, A. E., Lallemand, S. E., and Collot, J.-Y., 1998, A detailed study of the
247 Gagua Ridge: A fracture zone uplifted during a plate reorganisation in the
248 Mid-Eocene: *Marine Geophysical Researches*, v. 20, no. 5, p. 403-423,
249 doi:10.1023/A:1004650323183.
- 250 Deschamps, A., Monié, P., Lallemand, S., Hsu, S. K., and Yeh, K. Y., 2000, Evidence
251 for Early Cretaceous oceanic crust trapped in the Philippine Sea Plate: *Earth*

252 and Planetary Science Letters, v. 179, no. 3, p. 503-516,
253 doi:[https://doi.org/10.1016/S0012-821X\(00\)00136-9](https://doi.org/10.1016/S0012-821X(00)00136-9).

254 Dominguez, S., Lallemand, S., Malavieille, J., and Schnürle, P., 1998, Oblique
255 subduction of the Gagua Ridge beneath the Ryukyu accretionary wedge
256 system: Insights from marine observations and sandbox experiments: Marine
257 Geophysical Researches, v. 20, p. 383-402, doi:[10.1023/A:1004614506345](https://doi.org/10.1023/A:1004614506345).

258 Doo, W., Hsu, S.-K., Yeh, Y.-C., Tsai, C.-H., and Chang, C.-M., 2014, Age and
259 tectonic evolution of the northwest corner of the West Philippine Basin:
260 Marine Geophysical Research, v. 36, doi:[10.1007/s11001-014-9234-8](https://doi.org/10.1007/s11001-014-9234-8).

261 Eakin, D. H., McIntosh, K. D., Van Avendonk, H. J. A., and Lavier, L., 2015, New
262 geophysical constraints on a failed subduction initiation: The structure and
263 potential evolution of the Gagua Ridge and Huatung Basin: Geochemistry,
264 Geophysics, Geosystems, v. 16, no. 2, p. 380-400, doi:[10.1002/2014gc005548](https://doi.org/10.1002/2014gc005548).

265 Grimes, C. B., John, B., Kelemen, P., Mazdab, F. K., Wooden, J., Cheadle, M. J.,
266 Hanghoj, K., and Schwartz, J., 2007, Trace element chemistry of zircons from
267 oceanic crust: A method for distinguishing detrital zircon provenance: Geology,
268 v. 35, doi:[10.1130/G23603A.1](https://doi.org/10.1130/G23603A.1).

269 Hall, R., 2002, Cenozoic geological and plate tectonic evolution of SE Asia and the
270 SW Pacific: computer-based reconstructions, model and animations: Journal
271 of Asian Earth Sciences, v. 20, no. 4, p. 353-431,
272 doi:[https://doi.org/10.1016/S1367-9120\(01\)00069-4](https://doi.org/10.1016/S1367-9120(01)00069-4).

273 Hall, R, 2012, Late Jurassic–Cenozoic reconstructions of the Indonesian region and
274 the Indian Ocean: *Tectonophysics*, v. 570-571, p. 1-41,
275 doi:<https://doi.org/10.1016/j.tecto.2012.04.021>.

276 Hickey-Vargas, R., Bizimis, M., and Deschamps, A., 2008, Onset of the Indian Ocean
277 isotopic signature in the Philippine Sea Plate: Hf and Pb isotope evidence from
278 Early Cretaceous terranes: *Earth and Planetary Science Letters*, v. 268, no. 3, p.
279 255-267, doi:<https://doi.org/10.1016/j.epsl.2008.01.003>.

280 Hilde, T. W. C., and Lee, C.-S., 1984, Origin and evolution of the West Philippine
281 Basin: A new interpretation: *Tectonophysics*, v. 102, no. 1, p. 85-104,
282 doi:[https://doi.org/10.1016/0040-1951\(84\)90009-X](https://doi.org/10.1016/0040-1951(84)90009-X).

283 Hsieh, Y.-H., Liu, C.-S., Suppe, J., Byrne, T. B., and Lallemand, S., 2020, The Chimei
284 Submarine Canyon and Fan: A Record of Taiwan Arc-Continent Collision on
285 the Rapidly Deforming Overriding Plate: *Tectonics*, v. 39, no. 11, p.
286 e2020TC006148.

287 Hsu, S.-K., and Deffontaines, B., 2009, An introduction to geodynamics and active
288 tectonics in East Asia: *Tectonophysics*, v. 466, p. 135-139,
289 doi:[10.1016/j.tecto.2007.11.013](https://doi.org/10.1016/j.tecto.2007.11.013).

290 Huang, C.-Y., Wang, P., Yu, M., You, C.-F., Liu, C.-S., Zhao, X., Shao, L., Zhong, G.,
291 and Yumul, G. P., Jr, 2019, Potential role of strike-slip faults in opening up the
292 South China Sea: *National Science Review*, v. 6, no. 5, p. 891-901,
293 doi:[10.1093/nsr/nwz119](https://doi.org/10.1093/nsr/nwz119).

294 Ishizuka, O., Taylor, R. N., Milton, J. A., and Nesbitt, R. W., 2003, Fluid–mantle
295 interaction in an intra-oceanic arc: constraints from high-precision Pb isotopes:
296 Earth and Planetary Science Letters, v. 211, no. 3, p. 221-236,
297 doi:[https://doi.org/10.1016/S0012-821X\(03\)00201-2](https://doi.org/10.1016/S0012-821X(03)00201-2).

298 Kuo, B.-Y., Chi, W.-C., Lin, C.-R., Chang, E. T.-Y., Collins, J., and Liu, C.-S., 2009,
299 Two-station measurement of Rayleigh-wave phase velocities for the Huatung
300 basin, the westernmost Philippine Sea, with OBS: implications for regional
301 tectonics: Geophysical Journal International, v. 179, no. 3, p. 1859-1869,
302 doi:[10.1111/j.1365-246X.2009.04391.x](https://doi.org/10.1111/j.1365-246X.2009.04391.x).

303 Lallemand, S., 2016, Philippine Sea Plate inception, evolution, and consumption with
304 special emphasis on the early stages of Izu-Bonin-Mariana subduction:
305 Progress in Earth and Planetary Science, v. 3, no. 1, p. 15,
306 doi:[10.1186/s40645-016-0085-6](https://doi.org/10.1186/s40645-016-0085-6).

307 Li, X.-H., Li, Z.-X., and Li, W.-X., 2014, Detrital zircon U–Pb age and Hf isotope
308 constrains on the generation and reworking of Precambrian continental crust in
309 the Cathaysia Block, South China: A synthesis: Gondwana Research, v. 25, no.
310 3, p. 1202-1215, doi:<https://doi.org/10.1016/j.gr.2014.01.003>.

311 Mrozowski, C. L., Lewis, S. D., and Hayes, D. E., 1982, Complexities in the tectonic
312 evolution of the West Philippine Basin: Tectonophysics, v. 82, no. 1, p. 1-24,
313 doi:[https://doi.org/10.1016/0040-1951\(82\)90085-3](https://doi.org/10.1016/0040-1951(82)90085-3).

314 Plank, T., and Langmuir, C. H., 1998, The chemical composition of subducting

315 sediment and its consequences for the crust and mantle: *Chemical Geology*, v.
316 145, no. 3-4, p. 325-394, doi:Doi 10.1016/S0009-2541(97)00150-2.

317 Queano, K. L., Ali, J. R., Milsom, J., Aitchison, J. C., and Pubellier, M., 2007, North
318 Luzon and the Philippine Sea Plate motion model: Insights following
319 paleomagnetic, structural, and age-dating investigations: *Journal of*
320 *Geophysical Research: Solid Earth*, v. 112, no. B5,
321 doi:10.1029/2006jb004506.

322 Shao, W.-Y., Chung, S.-L., Chen, W.-S., Lee, H.-Y., and Xie, L.-W., 2015, Old
323 continental zircons from a young oceanic arc, eastern Taiwan: Implications for
324 Luzon subduction initiation and Asian accretionary orogeny: *Geology*, v. 43,
325 no. 6, p. 479-482, doi:10.1130/G36499.1.

326 Shervais, J. W., 1982, Ti-V plots and the petrogenesis of modern and ophiolitic lavas:
327 *Earth and Planetary Science Letters*, v. 59, no. 1, p. 101-118,
328 doi:[https://doi.org/10.1016/0012-821X\(82\)90120-0](https://doi.org/10.1016/0012-821X(82)90120-0).

329 Sibuet, J.-C., Hsu, S.-K., Le Pichon, X., Le Formal, J.-P., Reed, D., Moore, G., and
330 Liu, C.-S., 2002, East Asia plate tectonics since 15 Ma: constraints from the
331 Taiwan region: *Tectonophysics*, v. 344, no. 1, p. 103-134,
332 doi:[https://doi.org/10.1016/S0040-1951\(01\)00202-5](https://doi.org/10.1016/S0040-1951(01)00202-5).

333 Tani, K., Dunkley, D. J., and Ohara, Y., 2011, Termination of backarc spreading:
334 Zircon dating of a giant oceanic core complex: *Geology*, v. 39, no. 1, p. 47-50,
335 doi:10.1130/G31322.1.

336 Taylor, B., and Goodliffe, A. M., 2004, The West Philippine Basin and the initiation of
337 subduction, revisited: *Geophysical Research Letters*, v. 31, no. 12,
338 doi:10.1029/2004gl020136.

339 Wu, J., Suppe, J., Lu, R., and Kanda, R., 2016, Philippine Sea and East Asian plate
340 tectonics since 52 Ma constrained by new subducted slab reconstruction
341 methods: *Journal of Geophysical Research: Solid Earth*, v. 121, no. 6, p.
342 4670-4741, doi:10.1002/2016jb012923.

343 Xu, J., Ben-Avraham, Z., Kelty, T., and Yu, H.-S., 2014, Origin of marginal basins of
344 the NW Pacific and their plate tectonic reconstructions: *Earth-Science*
345 *Reviews*, v. 130, p. 154-196,
346 doi:<https://doi.org/10.1016/j.earscirev.2013.10.002>.

347 Yu, J.-H., O'Reilly, S. Y., Wang, L., Griffin, W. L., Zhou, M.-F., Zhang, M., and Shu,
348 L., 2010, Components and episodic growth of Precambrian crust in the
349 Cathaysia Block, South China: Evidence from U–Pb ages and Hf isotopes of
350 zircons in Neoproterozoic sediments: *Precambrian Research*, v. 181, no. 1, p.
351 97-114, doi:<https://doi.org/10.1016/j.precamres.2010.05.016>.

352 Zahirovic, S., Seton, M., and Müller, R. D., 2014, The Cretaceous and Cenozoic
353 tectonic evolution of Southeast Asia: *Solid Earth*, v. 5, no. 1, p. 227-273,
354 doi:10.5194/se-5-227-2014.

355 Zahirovic, S., Matthews, K. J., Flament, N., Müller, R. D., Hill, K. C., Seton, M., and
356 Gurnis, M., 2016, Tectonic evolution and deep mantle structure of the eastern

357 Tethys since the latest Jurassic: Earth-Science Reviews, v. 162, p. 293-337,

358 doi:<https://doi.org/10.1016/j.earscirev.2016.09.005>.

359

360 **FIGURE CAPTIONS**

361 **Fig. 1.** Geological map of the Gagua Ridge (GR) and adjacent regions. Red star,
362 sampling location of GR lavas; Black star, Taiwan Cathaysian continental fragment of
363 Shao et al. (2015).

364

365 **Fig. 2.** (A) ϵ_{Hf} (t) versus U-Pb age, (B) U-Pb age histogram, (C) Th versus U, (D)
366 U/Yb versus Y of zircons sampled from the Gagua Ridge (GR) lavas. For comparison,
367 the zircons from continental and oceanic crust, and mantle peridotite and kimberlite
368 (Grimes et al., 2007 and references therein), eastern Taiwan lavas (Shao et al., 2015)
369 and Cathaysia Block detrital zircons (Yu et al., 2010) are plotted. (E-F) $^{40}\text{Ar}/^{39}\text{Ar}$ age
370 spectrum for plagioclase from the GR lavas.

371

372 **Fig. 3.** (A) Variation of total alkali ($\text{Na}_2\text{O} + \text{K}_2\text{O}$) versus SiO_2 , (B) Primitive
373 mantle-normalized trace element pattern, (C) Ti-V discrimination diagram (Shervais,
374 1982), (D) Ba/Yb versus Nb/Yb, (E) $^{206}\text{Pb}/^{204}\text{Pb}$ versus Nd/Pb and (F-H) Isotopic
375 compositions of the Gagua Ridge (GR) lavas. The numbers adjacent to lines indicate
376 the % of slab-derived fluid added to the source mantle (See data sources and isotope
377 modeling details in Table DR5).

378

379 **Fig. 4.** Present-day Southeast Asia map showing possible tectonic journey of the
380 Cathaysian-affinity continental crustal sliver beneath the Gagua Ridge (GR) found in
381 this study (red star). The continental sliver (red polygon) rifted from South China
382 during the Cretaceous and possibly followed one of two paths: far-traveled (purple path)
383 or short transport (orange path). Brown areas show present-day landmasses; green area
384 shows present-day Huatung Basin (HB).

385

386 Supplemental Material. Methods, and supplemental figures and Tables. Please visit
387 [XX](#) to access the supplemental material.

Figure 1

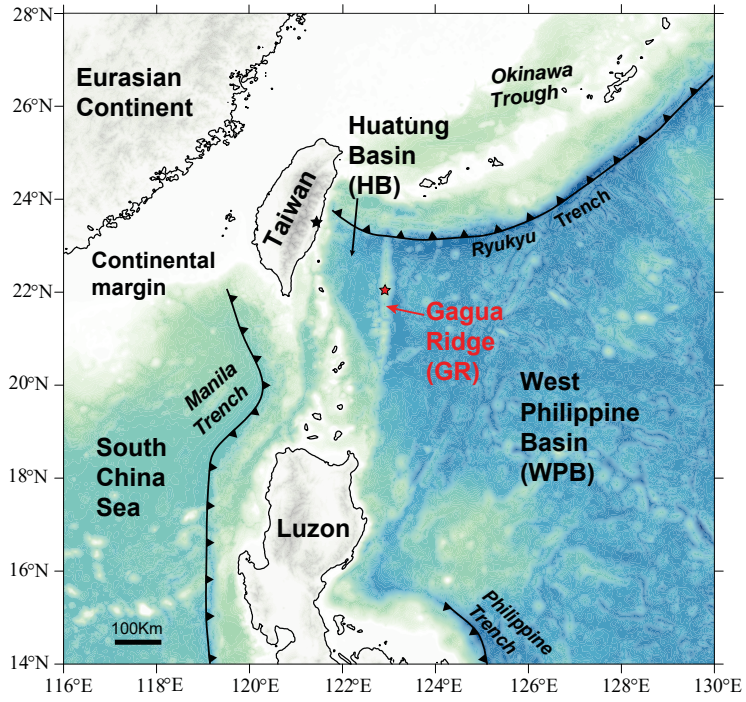


Figure 2

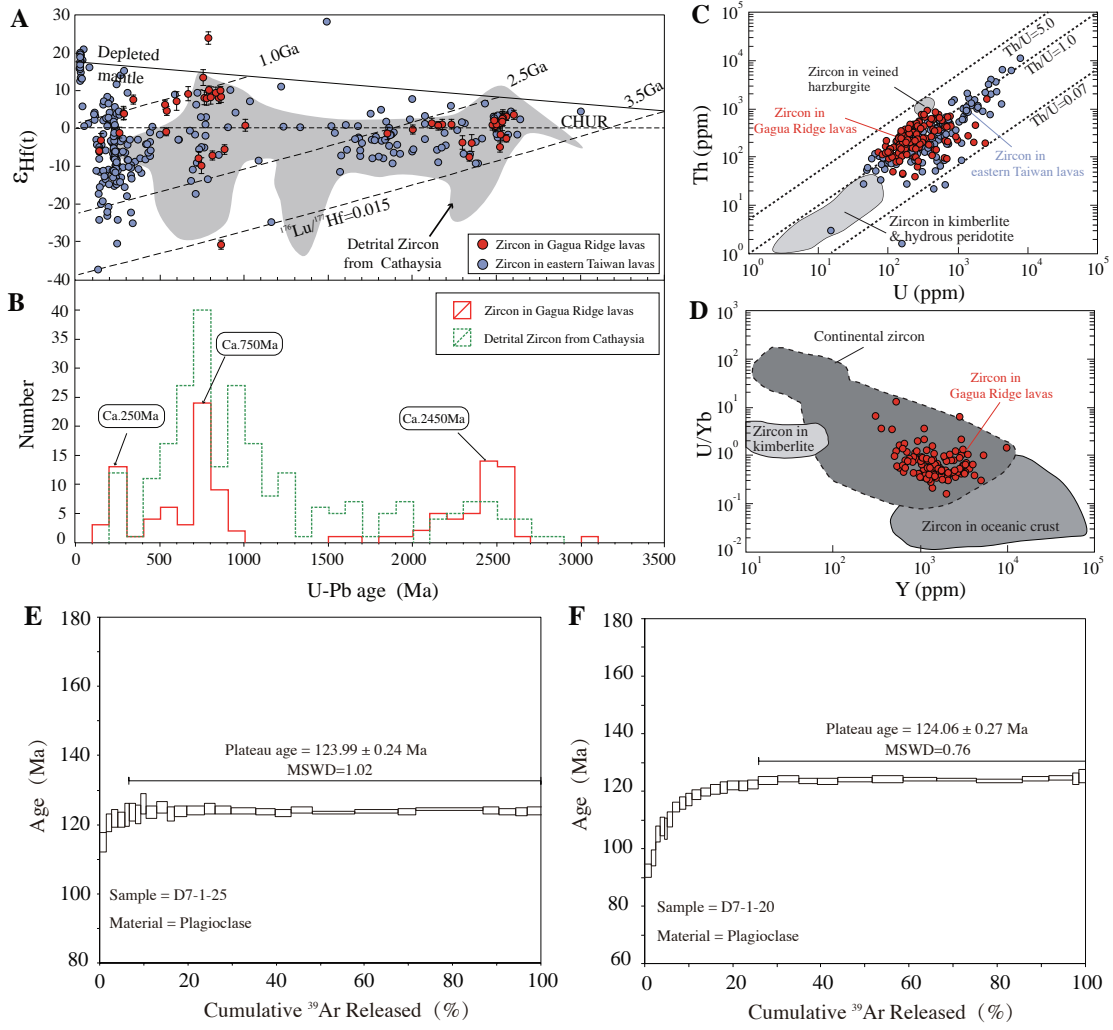


Figure 3

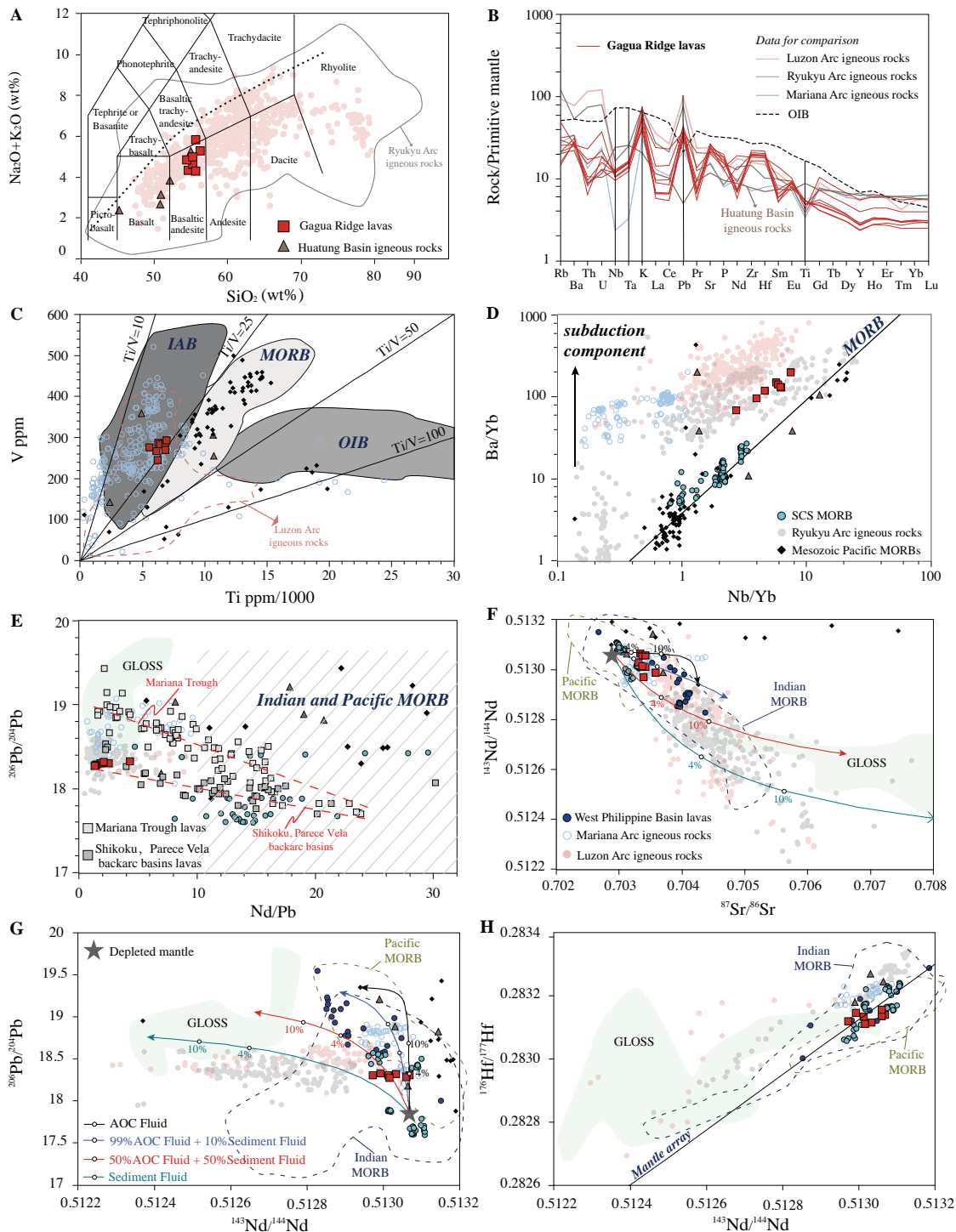


Figure 4

